

Linköping University Post Print

Test of the proximity force approximation

Bo E. Sernelius and C.E. Roman-Velazquez

N.B.: When citing this work, cite the original article.

Original Publication:

Bo E. Sernelius and C.E. Roman-Velazquez, Test of the proximity force approximation, 2009, Journal of Physics: Conference Series, (161), 012016.

<http://dx.doi.org/10.1088/1742-6596/161/1/012016>

Copyright: Institute of Physics

<http://journals.iop.org/>

Postprint available at: Linköping University Electronic Press

<http://urn.kb.se/resolve?urn=urn:nbn:se:liu:diva-21267>

Test of the Proximity Force Approximation

Bo E Sernelius and C E Román-Velázquez

Department of Physics, Chemistry, and Biology, Linköping University, SE-58183 Linköping, Sweden

E-mail: bos@ifm.liu.se

Abstract. We study the geometrical corrections to the simple Proximity Force Approximation (PFA) for the non-retarded Casimir force. We extend traditional PFA in two ways: We take the whole surfaces of the objects facing each other into account, not just the curvatures at the point of closest distance; we take the thickness of the coating of coated objects into account in the formalism. We present analytical and numerical results for a sphere above a substrate, for a spherical shell above a substrate, and for two interacting spheres. We compare the results to those from a multi-polar expansion method, a method based on a more solid foundation.

1. Introduction

J. D. van der Waals found empirically in 1873 that there is an attractive force between non-polar atoms. He studied the equation of state for real gases and found that there had to be a correction added to the pressure in the ideal-gas law. This indicated an attractive force between the gas atoms. It took a long time, until 1930, before there was an explanation to this force. London [1] gave the explanation in terms of fluctuations in the electron density within the atoms (fluctuating dipoles). In an alternative description [2] one may, instead of discussing the particles, focus on the electromagnetic fields. The force may be expressed as a result of changes in the zero-point energy of the electromagnetic normal modes of the system. There are modes associated with the atoms and modes associated with the vacuum. Casimir studied a more pure and idealized system consisting of two perfectly reflecting metal plates. In this geometry there are no modes associated with the plates themselves; there are only vacuum modes. The presence of the plates changes the vacuum modes and their zero-point energy. He published his findings in a classical paper [3] in 1948, the Casimir force was born, 60 years ago. Casimir's paper is one of the most important papers in the history of physics since it demonstrates that the boundary conditions of a system may change its zero-point energy and hence its properties. In the case of objects made from real materials both the modes associated with the objects and the vacuum modes contribute to the force [2]. The first type dominates in the van der Waals region which is for smaller separations. For larger separations between the objects the vacuum modes dominate and the result is the Casimir force. In the idealized case of perfect metals there is no van der Waals range. In 1997 Lamoreaux [4] performed the first modern high-precision measurements of the Casimir force. The accuracy was good enough to make the direct comparison with theory feasible. This spurred a burst of renewed interest in the Casimir effect.

On the theory side it may be complicated to calculate the force between objects of general shape. There are exceptions, though. The van der Waals and Casimir forces between half spaces is feasible to calculate. For finite objects at large distances one may use multipolar expansions

[5]. However, for small separations one needs to keep more and more terms in the expansion the smaller the distance; one reaches a limit when the method is no longer feasible to use.

In this work we study an approximation that comes handy in this situation. The Proximity Force Approximation (PFA). It was first used already in 1934 [6] in connection with coagulation of aerosols. It is a very powerful and widely used approximation for the interaction at short distances between two objects. Lamoreaux' experiment, discussed above, is interpreted within this approximation. It has also been used in the determination of surface roughness effects [7]. It is difficult to make a strict estimate of how good the approximation is since it is based on a very shaky foundation but it has gained a wide-spread acceptance in recent years.

The basic idea of the approximation is that the interaction potential between the objects is an average interaction energy between parallel planar interfaces,

$$V(z) = \int_S dS E_p(w), \quad (1)$$

where $E_p(w)$ is the interaction energy per unit area between planar interfaces a distance w apart. The variable z is the closest distance between the two objects. The surface S is not uniquely defined and the choice of S is in the general case not a trivial choice to make. In the examples we discuss here the choice is more obvious. For objects above a substrate we may choose S to be that part of a flat surface, parallel to the substrate, that is covered by the projection of the object; w is the distance at dS between the substrate and the object along the normal to S . In the case of two interacting objects we suggest that S is that part of the planar surface, perpendicular to the resulting force, where the projections of the two objects overlap; w is the distance at dS between the two objects along the normal to S .

Some attempts have been made to show its validity in different cases. However, the lack of a general and rigorous proof still remains, as well as estimates of the level of accuracy at all distances. In the present work we follow an alternative procedure. We extend the traditional PFA by taking the geometry into account in an optimal way. We produce both analytical and numerical results. The numerical results we compare to those from the multi-polar calculation method [5]. In this article we limit the results to those for a sphere above a substrate, for a spherical shell above a substrate, and for two interacting spheres. A more exhaustive study of the PFA results for a wide range of geometries and configurations will appear in a forthcoming publication [8].

We use extensions to the traditional PFA as discussed in Sec. 2. In Sec. 3 we show how the calculation of the interaction energy per unit area in planar structures are performed. These results are used as input in our PFA calculations. In Sec. 4 we give a general expression for the interaction energy for half spaces, cylinders and spheres. Sec. 5 is devoted to spherical objects, Finally, summary and conclusions are found in Sec. 6.

2. The Proximity Force Approximation in this work

Traditionally in the PFA of the interaction between two objects one only takes into consideration the surface of each object that is facing the other object. The function $E_p(w)$, in Eq. (1), is the energy per unit area for two half spaces, made up from the materials of the two objects, separated by the distance w . If the objects are immersed in an ambient medium the gap between the two half spaces is also filled with this medium. With this treatment the backsides of the objects have no effects at all. One gets, e.g., the same result for two spheres as for two halvespheres. We know that the normal modes contributing to the interaction may extend through the objects and continue on the other side. Thus, the backside may have important effects on the results. One may extend the treatment by using $E_p(w)$ from a planar structure with four interfaces instead of two. The distance between the interfaces surrounding the object material is the local thickness of the object. We will not consider this in the present work, but address another limitation that

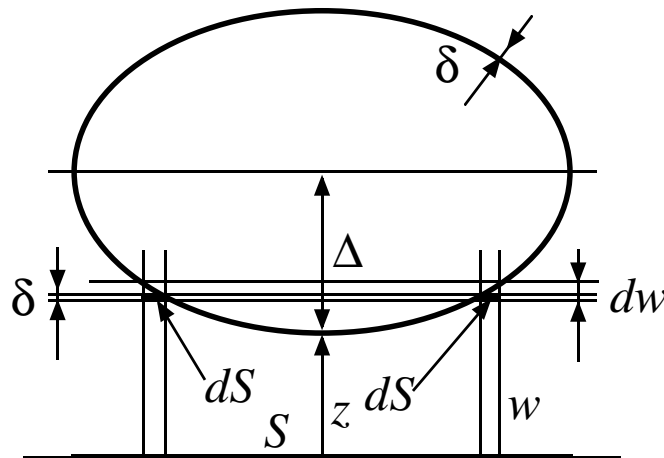


Figure 1. Coated oblate spheroid above a substrate used to illustrate the parameters discussed in the text.

is more severe. Two coated spheres, e.g., are in PFA treated as solid spheres. We will extend the treatment by considering a planar structure with four interfaces. In the most general case the two coatings are of different materials and of different thickness. We let $E_p(w, \delta)$ be the energy per unit area for two coated half spaces, made up from the materials of the two objects, separated the distance w . The thickness of the coating is denoted by δ . We may express the potential as

$$V(z) = \int_S dS E_p(w, \delta) = \int_z^{z+\Delta} dw \underbrace{\frac{dS}{dw}}_{g(w-z)} E_p(w, \delta), \quad (2)$$

and find the force as

$$F(z) = -\frac{dV}{dz} = -g(\Delta) E_p(z + \Delta, \delta) + g(0) E_p(z, \delta) - \int_z^{z+\Delta} dw \frac{dg(w-z)}{dz} E_p(w, \delta). \quad (3)$$

In many cases $g(\Delta)$ vanishes, like in the illustrating example in Fig. 1. Here we have a coated spheroid above a substrate. The surface S is defined through the projection of the object onto the substrate. When $g(\Delta)$ vanishes we have

$$F(z) = g(0) E_p(z, \delta) \left[1 + \frac{1}{g(0) E_p(z, \delta)} \int_z^{z+\Delta} dw \frac{d^2 S}{dw^2} E_p(w, \delta) \right], \quad (4)$$

where the first part is what one usually means with PFA. The remaining part, within brackets, is a correction factor depending on the geometry. This factor is often dropped without any motivation at all or with the argument that the resulting error is of the same order of magnitude as the error in PFA itself. Often $E_p(w, \delta)$ has a known power dependence in w over the whole integration interval. Then we may often find an analytical expression for the correction factor. In Fig. 1 we study a coated oblate spheroid above an uncoated substrate. The lowest horizontal line is the substrate boundary. The thicker part of this line indicates the surface S , which is defined by the projection of the spheroid on the substrate. The integration variable w varies from z , the closest distance, to $z + \Delta$. The region between w and $w + dw$ picks out a surface

on the object whose projection on the substrate is a ring of area dS . This surface contributes, in the PFA spirit, to the energy with dS times the energy per unit area, $E_p(w, \delta)$, of the planar configuration defined by the substrate and the film of thickness δ , indicated in the figure. If the spheroid is not an empty shell, the half space above the film should be filled by the material of the spheroid.

To summarize, in this work we extend the traditional PFA in two ways; we retain the correction factor of Eq. (4); we extend PFA to include the finite coat thickness of coated objects. The effects of these extensions are demonstrated and comparisons are made to numerical results from more accurate calculations. Throughout the text we refer to results from traditional PFA as PFA results and to extended or corrected PFA results as full PFA results.

Before we proceed with the various objects we derive, in next section, the interaction energy in those planar structures we need for the PFA calculations.

3. Planar structures

A general expression for the interaction energy per unit area in a planar system where only one of the distances, w , between neighboring interfaces is allowed to vary is [2]

$$\begin{aligned} E_p(w) &= \frac{\hbar}{2} \int_{-\infty}^{\infty} \frac{d\omega}{2\pi} \int \frac{d^2k}{(2\pi)^2} \{ \ln [f(\mathbf{k}, i\omega, w)] - \ln [f(\mathbf{k}, i\omega, \infty)] \} \\ &= \frac{\hbar}{2} \int_{-\infty}^{\infty} \frac{d\omega}{2\pi} \int \frac{d^2k}{(2\pi)^2} \ln \left[\frac{f(\mathbf{k}, i\omega, w)}{f(\mathbf{k}, i\omega, \infty)} \right], \end{aligned} \quad (5)$$

where the reference energy is set to when w is infinite. The variable \mathbf{k} is the two dimensional wave vector in the plane of the interfaces. The function $f(\mathbf{k}, \omega, w)$ is the function in the condition for having electromagnetic normal modes in the planar system,

$$f(\mathbf{k}, \omega, w) = 0. \quad (6)$$

In the general case there are two of these functions, one for TE modes and one for TM modes. Here we limit the treatment to the non-retarded limit. One of the effects from neglecting retardation is that the TE modes are absent. In the case of a coated object above a coated substrate or of two coated objects we need four interfaces between five regions. For a structure of the type 1|2|3|4|5 where medium 3 has the variable thickness w we have

$$\frac{f(\mathbf{k}, \omega, w)}{f(\mathbf{k}, \omega, \infty)} = 1 + e^{-2kw} \frac{r_{23}r_{34} + e^{-2kd_2}r_{12}r_{34} + e^{-2kd_4}r_{23}r_{45} + e^{-2kd_2}e^{-2kd_4}r_{12}r_{45}}{1 + e^{-2kd_2}r_{12}r_{23} + e^{-2kd_4}r_{34}r_{45} + e^{-2kd_2}e^{-2kd_4}r_{12}r_{23}r_{34}r_{45}}, \quad (7)$$

where $k = |\mathbf{k}|$ and

$$r_{ij} = \frac{\varepsilon_j(\omega) - \varepsilon_i(\omega)}{\varepsilon_j(\omega) + \varepsilon_i(\omega)}. \quad (8)$$

The function $\varepsilon_i(\omega)$ and d_i are the dielectric function and thickness, respectively, of region i . In the case of a coated object above a substrate or of two objects where only one is coated we need three interfaces between four regions. For a structure of the type 1|3|4|5 where medium 3 has the variable thickness w we let $r_{12} = 0$ and get

$$\frac{f(\mathbf{k}, \omega, w)}{f(\mathbf{k}, \omega, \infty)} = 1 + e^{-2kw} \frac{r_{13}r_{34} + e^{-2kd_4}r_{13}r_{45}}{1 + e^{-2kd_4}r_{34}r_{45}}. \quad (9)$$

In the case of an uncoated object above an uncoated substrate or of two uncoated objects we need two interfaces between three regions. For a structure of the type 1|3|5 where medium 3 has the variable thickness w we let $r_{45} = 0$ and get

$$\frac{f(\mathbf{k}, \omega, w)}{f(\mathbf{k}, \omega, \infty)} = 1 + e^{-2kw} r_{13}r_{35}. \quad (10)$$

For this last structure the integration over momentum in Eq. (5) may be performed and results in an infinite series.

$$\begin{aligned} E_p(w) &= \frac{\hbar}{8\pi^2} \int_{-\infty}^{\infty} d\omega \int_0^{\infty} dk k \ln \left[1 - e^{-2kw} r_{13} r_{53} \right] = \frac{\hbar}{32\pi^2 w^2} \int_{-\infty}^{\infty} d\omega \int_0^{\infty} dk k \ln \left[1 - e^{-k} r_{13} r_{53} \right] \\ &= -\frac{\hbar}{32\pi^2 w^2} \int_{-\infty}^{\infty} d\omega \sum_{l=1}^{\infty} \frac{(r_{13} r_{53})^l}{l^3} = -\frac{\hbar}{32\pi^2 w^2} \sum_{l=1}^{\infty} \frac{\langle \omega_l \rangle}{l^3}, \end{aligned} \quad (11)$$

where the characteristic dielectric integrals $\langle \omega_l \rangle$ are

$$\langle \omega_l \rangle = \int_{-\infty}^{\infty} d\omega \left[\frac{\varepsilon_1(\omega) - \varepsilon_3(\omega)}{\varepsilon_1(\omega) + \varepsilon_3(\omega)} \frac{\varepsilon_5(\omega) - \varepsilon_3(\omega)}{\varepsilon_5(\omega) + \varepsilon_3(\omega)} \right]^l. \quad (12)$$

This result is obtained after a variable substitution, series expansion of the logarithm, followed by the integration over momentum.

4. General expression for half spaces, cylinders and spheres

For solid objects in neglect of the geometrical correction in Eq. (4) one may find the following general expression for half spaces, cylinders and spheres: [2, 9]

$$E(z) = -\frac{\hbar}{32\pi^2 z^{(1+n/2)}} \Gamma(1+n/2) \left[\frac{2\pi R_1 R_2}{R_1 + R_2} \right]^{1-n/2} \sum_{l=1}^{\infty} \frac{\langle \omega_l \rangle}{l^3}, \quad (13)$$

where $n = 0$ for spheres, $n = 1$ for cylinders, and $n = 2$ for half spaces. The result is for the interaction energy in case of spheres, the interaction energy per unit length for cylinders and the interaction energy per unit area for half spaces. The variable z is the closest distance between the objects. Thus, for two half spaces we have

$$E(z) = -\frac{\hbar}{32\pi^2 z^2} \sum_{l=1}^{\infty} \frac{\langle \omega_l \rangle}{l^3} = E_p(z), \quad (14)$$

for two cylinders of radii R_1 and R_2

$$E(z) = -\frac{\hbar}{32\pi^2 z^{3/2}} \Gamma(3/2) \left[\frac{2\pi R_1 R_2}{R_1 + R_2} \right]^{1/2} \sum_{l=1}^{\infty} \frac{\langle \omega_l \rangle}{l^3} = \Gamma(3/2) \sqrt{\frac{2\pi R_1 R_2 z}{R_1 + R_2}} E_p(z), \quad (15)$$

and for two spheres of radii R_1 and R_2 the result is

$$E(z) = -\frac{\hbar}{32\pi^2 z} \left[\frac{2\pi R_1 R_2}{R_1 + R_2} \right] \sum_{l=1}^{\infty} \frac{\langle \omega_l \rangle}{l^3} = \left[\frac{2\pi R_1 R_2 z}{R_1 + R_2} \right] E_p(z). \quad (16)$$

To get the result for a cylinder of radius R above a substrate we let R_2 go to infinity and replace R_1 with R in Eq. (15). This results in

$$E(z) = -\frac{\hbar}{32\pi^2 z^{3/2}} \Gamma(3/2) \sqrt{2\pi R} \sum_{l=1}^{\infty} \frac{\langle \omega_l \rangle}{l^3} = \Gamma(3/2) \sqrt{2\pi R z} E_p(z). \quad (17)$$

To get the result for a sphere of radius R above a substrate we let R_2 go to infinity and replace R_1 with R in Eq. (16). This results in

$$E(z) = -\frac{\hbar}{32\pi^2 z} 2\pi R \sum_{l=1}^{\infty} \frac{\langle \omega_l \rangle}{l^3} = 2\pi R z E_p(z). \quad (18)$$

This is as far as we get with the general formula. Now, we continue in next and the following sections with the geometrical corrections for spherical objects.

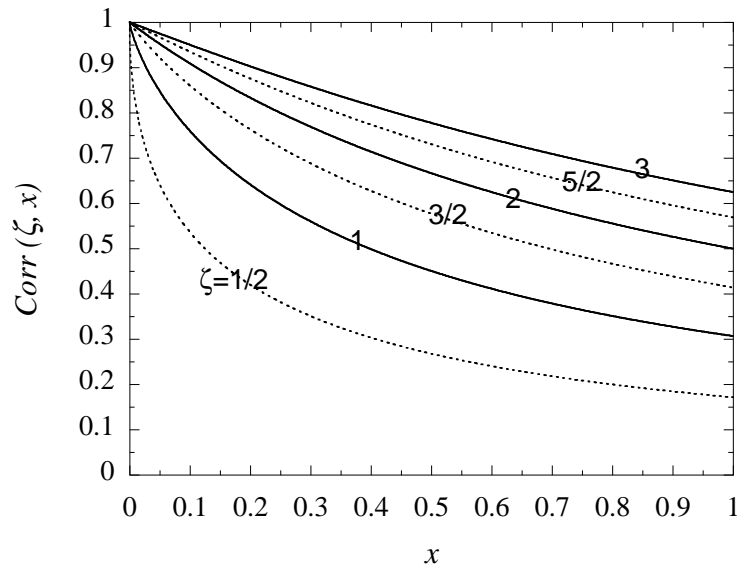


Figure 2. The correction factor $Corr(\zeta, x)$ for a set of ζ values.

5. Spherical objects

Spherical objects are often used in experiments. The advantage is that one avoids the problem of alignment. This is the case both for a sphere above a substrate and for two interacting spheres. In Lamoreaux's [4] classical measurement of the force between two gold plates one actually measured the force between a sphere and a planar surface.

5.1. Sphere-substrate interaction

For a sphere above a substrate the parameters entering Eq. (4) are

$$\Delta = R; \quad g(x) = 2\pi(R - x); \quad g(0) = 2\pi R; \quad \frac{d^2 S}{dw^2} = -2\pi, \quad (19)$$

and this results in

$$F(z) = 2\pi R E_p(z, \delta) \left[1 - \frac{1}{R E_p(z, \delta)} \int_z^{z+R} dw E_p(w, \delta) \right], \quad (20)$$

where we have included the possibility for the sphere and/or the substrate to have a coating of thickness δ . If $E_p(w, \delta)$ varies as

$$E_p(w, \delta) = -C/w^\zeta \quad (21)$$

in the whole integration interval we find the correction factor, $Corr(\zeta, x)$ on analytical form

$$Corr(\zeta, x) = \begin{cases} 1 - [x - x^\zeta / (1+x)^{\zeta-1}] / (\zeta - 1); & \zeta \neq 1 \\ 1 - x \ln[(1+x)/x]; & \zeta = 1 \end{cases} \quad (22)$$

where $x = z/R$. The correction factor is illustrated for some ζ values in Fig. 2. Eq. (20) is valid both in the non-retarded and retarded separation regions. The PFA is only good for small x -values but if R is big enough one may still be in the retarded region. For uncoated sphere

and substrate $\zeta = 2$ ($\zeta = 3$) in the non-retarded (retarded) region. If either of the sphere and substrate or both are coated the separation dependence is in general more complex. If a metallic coating is thin enough there is a separation range where $\zeta = 5/2$.

With the proper scaling one may produce universal figures, i.e., figures that are identical for all values of R . From Eqs. (5) and (7) follows that $E_p(w, \delta) = f(w/R, \delta/R)/w^2$. From Eq. (20) follows that if one plots $R \times F$ as a function of z/R the results look identical as long as the coat thickness is the same fraction of R . This means that there is no need to repeat the calculations for different sphere radii. In Fig. 3 we show R times the non-retarded force on a gold sphere above a gold substrate as function of normalized separation z/R . Throughout we use the dielectric function of gold given in Ref. [10]. The differences between the curves

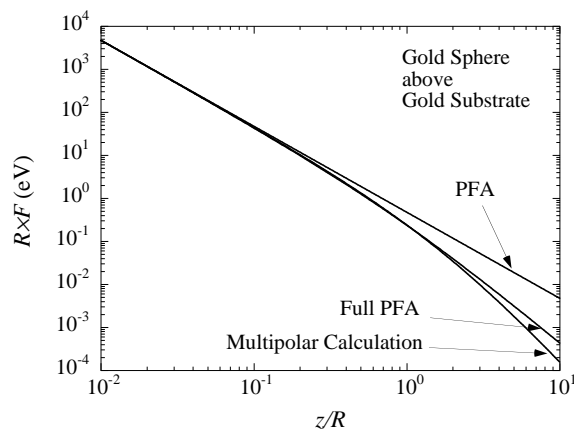


Figure 3. R times the non-retarded force on a gold sphere above a gold substrate as function of z/R for the multipolar result, the PFA result and the geometry corrected or full PFA result.

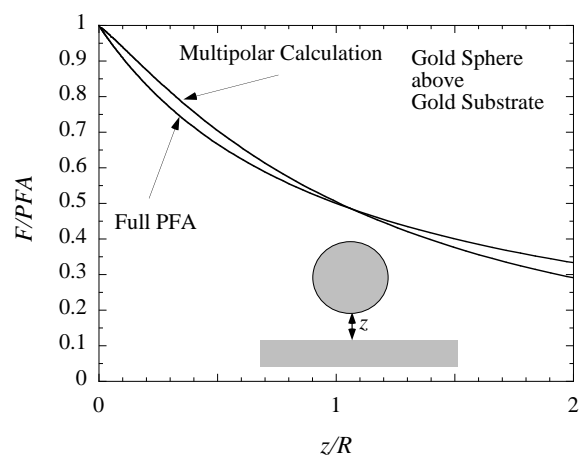


Figure 4. The non-retarded force on a gold sphere above a gold substrate relative the PFA result as function of z/R for the multipolar result and the full PFA result.

are not clearly seen in a figure like this. In Fig. 4 we show the result from the multipolar calculation and the geometry corrected or full PFA result relative the PFA result. In Fig. 5 we show R times the non-retarded force on a spherical gold shell above a gold substrate as function of normalized separation z/R . The thick solid curve and dashed curve are the PFA and full PFA curves, respectively, for a solid gold sphere and are the same as in Fig. 3; the solid curve with open circles is the result from the multipolar calculation for a shell of a thickness of one percent of the radius; the filled circles are our extended PFA result for the gold shell; the solid curve with triangles is our extended and full PFA result for the gold shell. We note that the full result, from the multipolar calculation, follows the PFA result for a solid gold sphere for distances smaller than approximately the coat thickness. Then for larger separations there is a region where it follows rather closely the 2D PFA result obtained by replacing the gold film with a 2D (two dimensional) metallic sheet with 2D electron density given as the projection of the 3D electron density of the film. These results are derived in Refs. [11, 12],

$$R \times F = 2\pi R^2 E_p(z) \approx 0.1556 \sqrt{n \hbar^2 e^2 / m_e} \sqrt{\delta / R} / (z/R)^{5/2}, \quad (23)$$

where n is the conduction electron density of gold.

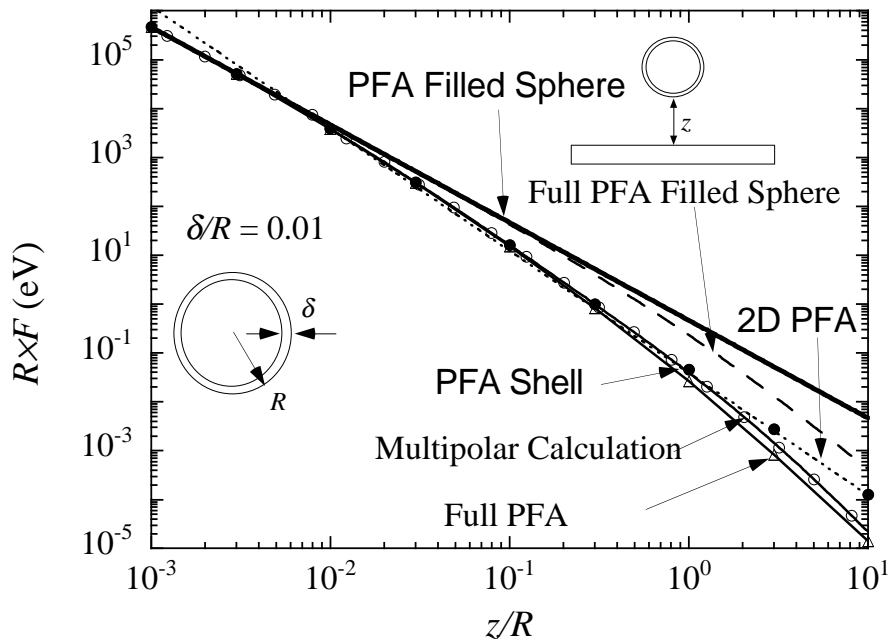


Figure 5. R times the non-retarded force on a spherical gold shell above a gold substrate as function of z/R . The curves are for the multipolar result (thin solid curve with open circles), the PFA result for a solid sphere (thick solid curve), the full PFA result for a solid sphere (dashed curve), the two-dimensional PFA result (dotted curve), the PFA result for the shell (solid circles) and the full PFA for the shell (triangles).

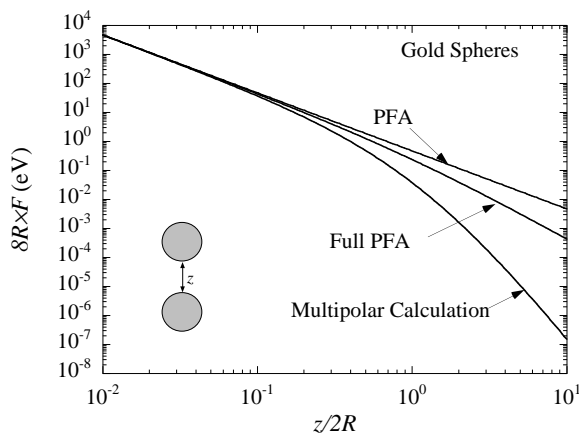


Figure 6. $8R$ times the non-retarded force between two gold spheres as function of $z/2R$ for the multipolar result, the PFA result and the full PFA result.

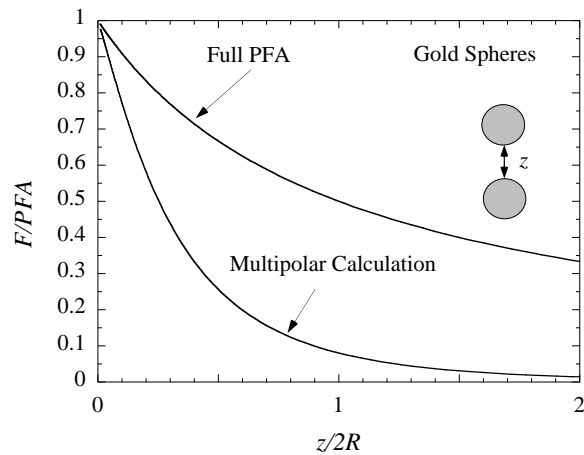


Figure 7. The non-retarded force between two equal size gold spheres relative the PFA result as function of $z/2R$ for the multipolar result and the full PFA result.

5.2. Sphere-sphere interaction

For two spheres of equal size the parameters entering Eq. (4) are

$$\Delta = 2R; \quad g(x) = \pi(R - x/2); \quad g(0) = \pi R; \quad \frac{d^2 S}{dw^2} = -\pi/2, \quad (24)$$

and this results in

$$F(z) = \pi R E_p(z, \delta) \left[1 - \frac{1}{2R E_p(z, \delta)} \int_z^{z+2R} dw E_p(w, \delta) \right]. \quad (25)$$

If $E_p(w, \delta)$ varies as in Eq. (21) in the whole integration interval we again find the correction factor, $Corr(\zeta, x)$, on analytical form and it is identical to the expression in Eq. (22) but now $x = z/2R$. In Fig. 6 we show $8R$ times the non-retarded force between two gold spheres of equal size as function of normalized separation $z/2R$. Plotted in this way the PFA and full PFA curves are identical to the corresponding ones in Fig. 3; the result from the multipolar calculation is not. In Fig. 7 we show the result from the multipolar calculation and the full PFA result relative the PFA result. We find that the agreement is not as good as in the case of a sphere above a substrate.

6. Summary and conclusions

In this work we have performed a critical test of the validity of the Proximity Force Approximation. This was done by comparisons with the results from a calculation method of more solid foundation, the multi-pole expansion method. Calculations were limited to a sphere above a substrate, a spherical shell above a substrate, and two interacting spheres. The results from a more extensive study will appear elsewhere [8].

We extended the traditional PFA in two ways; we did not just keep the small separation asymptote but took the geometrical shapes of the objects fully into account; we took the finite thickness of the coatings and free standing shells into account. For the three geometries studied in this work we found that the full PFA worked best for the shell above a substrate, second best for the solid sphere above a substrate, and third best for two interacting spheres.

In Fig. 1 we see that there are surface elements with high inclination angles. It would be tempting to try to improve and go beyond PFA by using element planes of variable inclination angle. However, the improvement is rudimentary. The angular dependence decreases rapidly with the ratio between the element distance to the substrate and the element-length.

Throughout this work we have presented universal figures, independent of the system scale. A word of caution is in place. All results are limited to the non-retarded range. This means that the range of validity in each figure depends on the scaling parameter. At the present status of the available measurement techniques one requires big enough objects, in the order of tens of micrometers, in close proximity, in the range of hundreds of nanometers. In a majority of cases this means that one is in the non-retarded limit and that the full PFA should be a good approximation.

References

- [1] London F 1930 *Z. Phys. Chem.* **B11** 222; 1930 *Z. Phys.* **63** 245
- [2] Sernelius Bo E 2001 *Surface Modes in Physics* (Berlin: Wiley-VCH)
- [3] Casimir H B G 1948 *Proc. Kon. Akad. Wet.* **51** 793
- [4] Lamoreaux S K 1997 *Phys. Rev. Lett.* **78** 5
- [5] Noguez C, Román-Velázquez C E, Esquivel-Sirvent R, and Villarreal C 2004 *Europhys. Lett.* **67** 191
- [6] Derjaguin B 1934 *Kolloid Z.* **69** 155
- [7] Genet C, Lambrecht A, Maia Neto P, and Reynaud S 2003 *Europhys. Lett.* **62** 484
- [8] Sernelius Bo E and Román-Velázquez C E, to be published
- [9] Langbein D 1974 *Theory of the Van der Waals Attraction* (New York: Springer) in the series *Springer Tracts in Modern Physics*
- [10] Lambrecht A and Reynaud S 2000 *Europhys. J.* **D8** 309
- [11] Boström M and Sernelius Bo E 2000 *Phys. Rev.* **B61** 2204
- [12] Sernelius Bo E and Björk P 1998 *Phys. Rev.* **B57** 6592